

# Complete Reconstitution of the Vancomycin-Intermediate *Staphylococcus aureus* Phenotype of Strain Mu50 in Vancomycin-Susceptible *S. aureus*

Yuki Katayama,<sup>a</sup> Miwa Sekine,<sup>a</sup> Tomomi Hishinuma,<sup>a</sup> Yoshifumi Aiba,<sup>b</sup> Keiichi Hiramatsu<sup>b</sup>

Department of Microbiology, Faculty of Medicine,<sup>a</sup> and Research Centre for Infection Control Science,<sup>b</sup> Juntendo University, Tokyo, Japan

**Complete reconstitution of the vancomycin-intermediate *Staphylococcus aureus* (VISA) phenotype of strain Mu50 was achieved by sequentially introducing mutations into six genes of vancomycin-susceptible *S. aureus* (VSSA) strain N315ΔIP. The six mutated genes were detected in VISA strain Mu50 but not in N315ΔIP. Introduction of the mutation Ser329Leu into *vraS*, encoding the sensor histidine kinase of the *vraSR* two-component regulatory (TCR) system, and another mutation, Glu146Lys, into *msrR*, belonging to the LytR-CpsA-Psr (LCP) family, increased the level of vancomycin resistance to that detected in heterogeneous vancomycin-intermediate *S. aureus* (hVISA) strain Mu3. Introduction of two more mutations, Asn197Ser into *graR* of the *graSR* TCR system and His481Tyr into *rpoB*, encoding the β subunit of RNA polymerase, converted the hVISA strain into a VISA strain with the same level of vancomycin resistance as Mu50. Surprisingly, however, the constructed quadruple mutant strain ΔIP4 did not have a thickened cell wall, a cardinal feature of the VISA phenotype. Subsequent study showed that cell wall thickening was an inducible phenotype in the mutant strain, whereas it was a constitutive one in Mu50. Finally, introduction of the Ala297Val mutation into *fdh2*, which encodes a putative formate dehydrogenase, or a 67-amino-acid sequence deletion into *sle1* [*sle1*(Δ67aa)], encoding the hydrolase of *N*-acetylmuramyl-L-alanine amidase in the peptidoglycan, converted inducible cell wall thickening into constitutive cell wall thickening. *sle1*(Δ67aa) was found to cause a drastic decrease in autolysis activity. Thus, all six mutated genes required for acquisition of the VISA phenotype were directly or indirectly involved in the regulation of cell physiology. The VISA phenotype seemed to be achieved through multiple genetic events accompanying drastic changes in cell physiology.**

Studies on the genetic mechanism of vancomycin-intermediate resistance revealed that it is acquired by *Staphylococcus aureus* through multistep mutations of the genes that are involved in the regulation of cell physiology (1–6). When exposed to cell wall synthesis inhibitors, *S. aureus* upregulates cell wall synthesis through the activation of the *vraSR* two-component regulatory (TCR) system (7–9). We previously reported that not only vancomycin but also β-lactam antibiotics, such as imipenem, can select for heterogeneous vancomycin-intermediate *S. aureus* (hVISA) mutants from a vancomycin-susceptible *S. aureus* (VSSA) strain, N315ΔIP (ΔIP) (10). In fact, such selection of hVISA by exposure to β-lactam antibiotics occurred in Japanese hospitals before the clinical introduction of vancomycin (11). Enhanced cell wall synthesis was observed in clinically isolated hVISA strain Mu3 as well as in hVISA strain ΔIP1 (previously designated strain ΔIP-H14 [9]) obtained *in vitro* by selection with imipenem at 8 μg/ml (10). Both strains had mutations in the *vraS* gene, encoding the sensor histidine kinase, which brought about the constitutive expression of the response regulator *vraR* and more than 50 genes which are under the control of the TCR system. The transcription of many genes involved in cell wall synthesis was found to be significantly augmented (9, 10). Therefore, the upregulation of cell wall synthesis caused by activation of the *vraSR* TCR system definitely contributes to vancomycin resistance. Clinical hVISA strain Mu3 and laboratory strain ΔIP1 carry different *vraS* mutations: the Ile5Asn (I5N) mutation in *vraS* [*vraS*(I5N)] and the Ser329Leu (S329L) mutation in *vraS* [*vraS*(S329L)]. However, the mutations had the same effect, i.e., constitutive activation of *vraSR* and up-regulation of the genes involved in cell wall synthesis (10).

Such *vraS* mutations are frequently observed in hVISA strains

in Japan (12) and may represent first-step mutations leading to the acquisition of the VISA phenotype (10, 13, 14). In a search for the next genetic events leading to the VISA phenotype, we determined and compared the whole-genome sequences of hVISA strain Mu3 and VISA strain Mu50 (15, 16). Nine Mu50-specific non-synonymous mutations were identified, and among these we found regulator mutation Asn197Ser (N197S) in *graR* [*graR*(N197S)], encoding TCR and the response to host defense peptide systems (16, 17). Introduction and overexpression of the mutated *graR* gene in Mu3 increased the level of vancomycin resistance to that in VISA strains (16). However, the level of vancomycin resistance of Mu3 established by introduction of a single copy of *graR*(N197S) by gene replacement increased the vancomycin MIC, but the strain did not attain the level of resistance defined for vancomycin-intermediate resistance (MIC ≥ 4 μg/ml) (18). We then examined another Mu50-specific mutation, His481Tyr (H481Y) in *rpoB*

Received 22 February 2016 Returned for modification 14 March 2016

Accepted 1 April 2016

Accepted manuscript posted online 11 April 2016

Citation Katayama Y, Sekine M, Hishinuma T, Aiba Y, Hiramatsu K. 2016. Complete reconstitution of the vancomycin-intermediate *Staphylococcus aureus* phenotype of strain Mu50 in vancomycin-susceptible *S. aureus*. *Antimicrob Agents Chemother* 60:3730–3742. doi:10.1128/AAC.00420-16.

Address correspondence to Yuki Katayama, yukkk@juntendo.ac.jp.

Supplemental material for this article may be found at <http://dx.doi.org/10.1128/AAC.00420-16>.

Copyright © 2016 Katayama et al. This is an open-access article distributed under the terms of the [Creative Commons Attribution 4.0 International license](https://creativecommons.org/licenses/by/4.0/).

[*rpoB*(H481Y)], encoding the  $\beta$  subunit of RNA polymerase. We found that introduction of the mutated *rpoB* together with *graR*(N197S) into Mu3 increased its vancomycin MIC to 8  $\mu$ g/ml, equivalent to that for Mu50 (18). We have already suggested that the *rpoB* mutation is one of the regulatory mutations increasing the level of resistance to vancomycin, daptomycin, and  $\beta$ -lactams (6, 18–22).

Here, we planned to reconstitute the entire VISA phenotype in a naive vancomycin-susceptible methicillin-resistant *S. aureus* (MRSA) strain which had not been exposed to vancomycin. For this project, we chose laboratory strain N315 $\Delta$ IP ( $\Delta$ IP), a laboratory derivative of clinical pre-MRSA strain N315 in which *mecl* was inactivated and the plasmid carrying the gene for penicillinase (PCase;  $\beta$ -lactamase) was eliminated. N315 represents the dominant health care-associated (HA) MRSA strain that has the same sequence type (ST5) as strains Mu3 and Mu50. N315 was isolated in 1982 prior to the clinical introduction of vancomycin in 1991 (11).  $\Delta$ IP was constructed to mimic Mu3 and Mu50, which have no PCase plasmid and in which the *mecl* genes are inactivated by mutation (23). We constructed a triple mutant strain of  $\Delta$ IP1 by introducing the three mutations *graR*(N197S), *rpoB*(H481Y), and *vraS*(S329L). Contrary to our expectation, however, this strain did not express VISA phenotype.

The Glu146Lys (E146K) mutation in *msr* [*msr*(E146K)] was previously shown to lower the imipenem MIC and teicoplanin resistance when it was overexpressed in VSSA strain N315 (3). The *msrR* gene is present on the *S. aureus* chromosome as one of the three paralogs encoding proteins of the LytR-CpsA-Psr (LCP) family (24). *msrR* (or *lcpA*) and the other two *lcp* genes, *lcpB* and *lcpC*, are proposed to function in the last stage of wall teichoic acid (WTA) synthesis, namely, in the attachment of teichoic acid to peptidoglycan (PG) (24, 25). WTA is proposed to control the autolysis of *S. aureus* cells through the stabilization of autolysin (26). However, it is not yet clear how the altered MsrR in Mu3 and Mu50 contributes to the rise in vancomycin resistance.

We have already reported that the Ala297Val (A297V) mutation in *fdh2* [*fdh2*(A297V)], encoding a putative mutated formate dehydrogenase, is responsible for resistance to vancomycin (6). The deletion of a 67-amino-acid sequence ( $\Delta$ 67aa) from the *lysM* domain in the *sle1* gene [*sle1*( $\Delta$ 67aa)], encoding the hydrolase of *N*-acetylmuramyl-L-alanine amidase in the peptidoglycan, was also found in Mu50 (3). It has been reported that the localization of Sle1 to the cross wall is abolished in staphylococcal *tagO* mutants, which are defective for WTA synthesis (27, 28). The teichoic acids regulate peptidoglycan cross-linking through the control of PBP 4 activity (29). We previously reported that the *tagO*, *cmk*, or *rpoB* mutation was found in a VISA strain obtained from an hVISA strain (6, 18). It was suggested that the altered teichoic acid synthesis, reduced peptidoglycan cross-linking, and upregulated cell wall synthesis by the UTP pool are closely associated with the VISA phenotype (1, 30, 31). We identified two novel mutations, *msrR*(E146K) and *sle1*( $\Delta$ 64aa), associated with WTA synthesis that were required for the complete reconstitution of the VISA phenotype of Mu50.

## MATERIALS AND METHODS

**Bacterial strains, plasmids, growth conditions, and determination of doubling time.** The *Staphylococcus* strains and plasmids used in the present study are listed in Table 1. The cloning and transformation of *Escherichia coli* DH5 $\alpha$  were carried out by standard techniques (TaKaRa-Bio

Co., Ltd., Shiga, Japan). All *S. aureus* strains were cultivated in brain heart infusion (BHI) broth or agar (Difco Laboratories, Detroit, MI) with aeration at 37°C, unless indicated otherwise. The antibiotics tetracycline and chloramphenicol (Sigma Chemical Co., St. Louis, MO) were used for the selection of the *S. aureus* transformants. The doubling time was calculated as described previously (19). The growth conditions were 37°C with shaking at 25 rpm in a TN-2612 incubator (Advantec, Tokyo, Japan). The optical density at 660 nm (OD<sub>660</sub>) versus time was plotted for each strain in the exponential growth phase.

**Antibiotic susceptibility tests.** Antibiotic susceptibility was examined by Etest (AB Biodisk, Solna, Sweden) and population analysis as described previously (32). All examinations were performed by using BHI broth or agar.

**DNA methods.** DNA manipulations were performed by standard methods (33). Restriction enzymes were used as recommended by the manufacturer (TaKaRa). Routine PCR amplification was performed with an Expand high-fidelity system (Roche, Mannheim, Germany).

**Construction of  $\Delta$ IP and  $\Delta$ IP1 mutants carrying *msrR*(E146K), *graR*(N197S), *fdh2*(A297V), and *sle1*( $\Delta$ 67aa).** All mutants tested in this study are described in Tables 1 and 2. For replacement of the asparagine amino acid residue at position 197 in *graR* with serine, replacement of the glutamate at position 146 in *msrR* with lysine, and replacement of the alanine at position 297 in *fdh* (*sa2102*) with valine, we used the pKOR1 allele replacement system, as described previously (10, 34). In brief, 1.0 kb of *graR*, *msrR*, or *sle1* insert DNA encompassing 1-kb flanking sequences of the phage attachment sites was generated by PCR from the chromosomal DNA of strain Mu50 (Table 3). The resulting plasmids, pKO-*graR*(N197S) pKO-*msrR*(E146K), and pKO- $\Delta$ *sle1*, were introduced into *S. aureus* by electroporation. pKO-*fdh*(A297V) has been reported by Matsuo et al. (6). Replacement of the *graR*(N197S) and *msrR*(E146K) gene alleles with wild-type *graR* and *msrR*, respectively, in  $\Delta$ IP or  $\Delta$ IP1 was carried out by a two-step procedure, as described previously (10).

**Growth curve and doubling time.** A total of 10<sup>5</sup> CFU of the preculture was inoculated into 10 ml of BHI broth and incubated at 37°C with shaking at 25 rpm in a model TN-2612 incubator (Advantec). The doubling time was calculated from the slope of the line obtained from a semilogarithmic graph of the growth curve. The log<sub>2</sub> OD<sub>660</sub> versus time was plotted for each strain in the exponential growth phase. The doubling time was calculated by the following formula:  $[(t_2 - t_1) \times \log_2] / (\log_2 \text{OD}_{660} \text{ at } t_2 - \log_2 \text{OD}_{660} \text{ at } t_1)$ , where  $t_2$  and  $t_1$  are the times at the end and the start of the logarithmic growth phase, respectively. The doubling time was measured in at least three independent experiments.

**Isolation of a rifampin-resistant mutant strain carrying *rpoB*(H481Y).** Twenty rifampin-resistant isolates were obtained from each of seven strains, strains  $\Delta$ IP,  $\Delta$ IP-m,  $\Delta$ IP-g,  $\Delta$ IP1,  $\Delta$ IP1-g,  $\Delta$ IP2, and  $\Delta$ IP3, by selection with BHI agar containing 1  $\mu$ g/ml of rifampin at frequencies of  $1.4 \times 10^{-7}$ ,  $3.0 \times 10^{-8}$ ,  $4.0 \times 10^{-8}$ ,  $8.0 \times 10^{-7}$ ,  $6.4 \times 10^{-8}$ ,  $6.5 \times 10^{-8}$ , and  $9.4 \times 10^{-8}$ , respectively. The nucleotide sequences of the *rpoB* genes from the resulting 20 rifampin-resistant isolates were determined by sequencing analysis.

**Transmission electron microscopy.** The preparation of *S. aureus* cells for transmission electron microscopy and examination of the cells by transmission electron microscopy were performed as described previously (1, 17). At least 100 cells cut nearly equatorially were measured for the evaluation of cell wall thickness, and the results are expressed as the means  $\pm$  standard deviations.

**Autolysis assay.** Triton X-100-stimulated autolysin activity in Tris-HCl buffer (pH 7.5) was measured as described previously (35). Cells were grown to the mid-exponential phase to an OD<sub>660</sub> of about 1.5 at a cultivation temperature of 37°C. The culture was rapidly chilled, and the cells were washed twice with ice-cold distilled water and suspended to an OD<sub>660</sub> of 2.0 in 50 mM Tris-HCl buffer supplemented with 0.05% Triton X-100. Autolytic activity was measured during incubation at 30°C as a decrease in the OD<sub>660</sub> by using a biophotorecorder (Advantec). All data from the autolysis experiments are reported as percentages of the initial

TABLE 1 Bacterial strains used in this study<sup>a</sup>

Strain	Description and relevant phenotype	Reference or source
Clinically isolated strains		
Mu50	VISA clinical strain with <i>vraS</i> (I5N), <i>msrR</i> (E146K), <i>graR</i> (N197S), <i>rpoB</i> (H481Y), and <i>fdh2</i> (A297V) mutations	13
Mu3	hVISA clinical strain with <i>vraS</i> (I5N) and <i>msrR</i> (E146K) mutations	13
Control strains		
N315	Pre-MRSA clinical strain carrying a functional <i>mecI</i> gene encoding the <i>mecA</i> gene transcription repressor; hetero-Met <sup>r</sup>	22
ΔIP	N315ΔIP, N315-derived laboratory strain, <i>mecI::tetL</i> , cured of PCase plasmid; hetero-Met <sup>r</sup> Tet <sup>r</sup>	22
ΔIP1	ΔIP-derived strain with <i>vraS</i> (S329L) mutation formerly designated ΔIP-H14; hVISA homo-Met <sup>r</sup> Tet <sup>r</sup>	9, 10
Δ <i>msrR</i> derivatives		
ΔIP Δ <i>msrR</i>	<i>msrR</i> -null mutant obtained from ΔIP; homo-Met <sup>r</sup> Tet <sup>r</sup>	This study
ΔIP1 Δ <i>msrR</i>	<i>msrR</i> -null mutant obtained from ΔIP1; homo-Met <sup>r</sup> Tet <sup>r</sup>	This study
ΔIP derivatives with wild-type <i>vraS</i>		
ΔIP-m	<i>msrR</i> (E146K) mutant obtained by gene replacement from ΔIP; Tet <sup>r</sup>	This study
ΔIP-mr	<i>rpoB</i> (H481Y) mutant obtained by rifampin selection of ΔIP-m; Rif <sup>r</sup> Tet <sup>r</sup>	This study
ΔIP-g	<i>graR</i> (N197S) mutant obtained by gene replacement from ΔIP; Tet <sup>r</sup>	This study
ΔIP-r	<i>rpoB</i> (H481Y) mutant obtained by rifampin selection of ΔIP; Rif <sup>r</sup> Tet <sup>r</sup>	10
ΔIP-gr	<i>rpoB</i> (H481Y) mutant obtained by rifampin selection of ΔIP-g; Rif <sup>r</sup> Tet <sup>r</sup>	This study
ΔIP1 derivatives carrying <i>vraS</i> (S329L)		
ΔIP1-g	<i>graR</i> (N197S) mutant obtained by gene replacement from ΔIP1; homo-Met <sup>r</sup> Tet <sup>r</sup>	This study
ΔIP1-r	<i>rpoB</i> (H481Y) mutant obtained by rifampin selection of ΔIP1; homo-Met <sup>r</sup> Tet <sup>r</sup>	10
ΔIP1-gr	<i>rpoB</i> (H481Y) mutant obtained by rifampin selection of ΔIP1-g; homo-Met <sup>r</sup> Rif <sup>r</sup> Tet <sup>r</sup>	This study
ΔIP2	<i>msrR</i> (E146K) mutant obtained by gene replacement from ΔIP1; homo-Met <sup>r</sup> Tet <sup>r</sup>	This study
ΔIP2 derivatives carrying both <i>vraS</i> (S329L) and <i>msrR</i> (E146K)		
ΔIP2-r	<i>rpoB</i> (H481Y) mutant obtained by rifampin selection of ΔIP2; homo-Met <sup>r</sup> Rif <sup>r</sup> Tet <sup>r</sup>	This study
ΔIP3	<i>graR</i> (N197S) mutant obtained by gene replacement from ΔIP2; homo-Met <sup>r</sup> Tet <sup>r</sup>	This study
ΔIP4	<i>rpoB</i> (H481Y) mutant obtained by rifampin selection of ΔIP3; homo-Met <sup>r</sup> Rif <sup>r</sup> Tet <sup>r</sup>	This study
ΔIP4-s	<i>sle1</i> (Δ67aa) mutant obtained by rifampin selection of ΔIP4; homo-Met <sup>r</sup> Rif <sup>r</sup> Tet <sup>r</sup>	This study
ΔIP5	<i>fdh2</i> (A297V) <sup>b</sup> mutant obtained by gene replacement from ΔIP4; homo-Met <sup>r</sup> Rif <sup>r</sup> Tet <sup>r</sup>	This study
ΔIP6	<i>sle1</i> (Δ67aa) mutant obtained by gene replacement from ΔIP5; homo-Met <sup>r</sup> Rif <sup>r</sup> Tet <sup>r</sup>	This study

<sup>a</sup> Abbreviations: m, *msrR*(E146K); g, *graR*(N197S); r, *rpoB*(H481Y); s, *sle1*(Δ67aa); Met<sup>s</sup>, methicillin susceptible; Met<sup>r</sup>, methicillin resistant; Tet<sup>r</sup>, tetracycline resistant; Rif<sup>r</sup>, rifampin resistant.

<sup>b</sup> *fdh2*, encoding a putative formyl dehydrogenase, corresponds to the open reading frames SA2102 of N315 and SAV2039 of Mu50.

turbidity (at zero time) and are representative of those from three independent experiments.

**RNA preparation and microarray analysis.** RNA extraction, cDNA labeling, hybridization, and volcano plot analysis performed by microarray analysis were carried out according to protocols described previously (19). Using the three normalized signal intensities, the statistical significance of the data was evaluated by Student's *t* test. Ratios of the fold change were calculated by using the average of the normalized signal intensity. Volcano plot analysis was performed as described previously (19), and plots were constructed by plotting the negative log<sub>10</sub> of the *P* value obtained by the *t* test on the *y* axis and the log<sub>2</sub> value of the fold change on the *x* axis.

**Statistical analysis.** The two-by-two contingency tables were evaluated by Fisher's exact test.

**Microarray data accession numbers.** The transcriptional profiles were published in NCBI under GEO accession number [GSE43643](https://www.ncbi.nlm.nih.gov/geo/query/acc.cgi?acc=GSE43643).

## RESULTS

**Properties of ΔIP-derived strains into which *vraS*, *graR*, and *rpoB* mutations are sequentially introduced.** To recreate the VISA phenotype of Mu50, ΔIP-derived strains were constructed by sequentially replacing the *vraS*, *graR*, and *rpoB* genes of ΔIP by their mutated counterparts from Mu50. The *vraS* and *graR* genes of ΔIP were replaced with mutated *vraS* and *graR* by an allele replacement procedure, and *rpoB*(H481Y) was incorporated by rifampin selection. The antibiograms of the strains were determined by Etest (Table 2). We have already reported that strain ΔIP1 has increased vancomycin resistance, and a typical population curve for the hVISA strain is shown in Fig. 1 (10). The replacement of the *graR* and *rpoB* genes in clinical hVISA strain Mu3 with *graR*(N197S) and *rpoB*(H481Y) converted Mu3 into a VISA strain

TABLE 2 Genotypes and antibiograms of  $\Delta$ IIP and  $\Delta$ IIP-derived mutant strains compared with those of Mu3 and Mu50

Strain <sup>a</sup>	Genotype <sup>b</sup>						MIC ( $\mu$ g/ml) of <sup>c</sup> :							VAN phenotype <sup>d</sup>
	<i>vraS</i>	<i>msrR</i>	<i>graR</i>	<i>rpoB</i>	<i>fdh2</i>	<i>sle1</i>	VAN	TEC	RIF	OXA	IPM	DAP	LZD	
Clinically isolated strains														
Mu50	I5N	E146K	N197S	H481Y	A297V	$\Delta$ 67aa <sup>e</sup>	12	12	>32	>256	>32	3	0.5	VISA
Mu3	I5N	E146K	—	—	—	—	3	24	0.006	>256	>32	2	0.75	hVISA
Control strains														
$\Delta$ IIP	—	—	—	—	—	—	1	1	0.004	6	0.75	0.75	1	VSSA
$\Delta$ IIP1	S329L	—	—	—	—	—	2	8	0.004	>256	>32	2	0.75	hVISA
$\Delta$ <i>msrR</i> derivatives														
$\Delta$ IIP $\Delta$ <i>msrR</i>	—	Deletion	—	—	—	—	1	0.75	0.004	2	0.19	1	0.75	VSSA
$\Delta$ IIP1 $\Delta$ <i>msrR</i>	S329L	Deletion	—	—	—	—	2	8	0.004	64	>32	2	0.5	hVISA
$\Delta$ IIP derivatives with wild-type <i>vraS</i>														
$\Delta$ IIP-g	—	—	N197S	—	—	—	1	0.75	0.006	6	0.38	1.5	1	VSSA
$\Delta$ IIP-r	—	—	—	H481Y	—	—	1	1	>32	5	1	0.5	0.5	VSSA
$\Delta$ IIP-gr	—	—	N197S	H481Y	—	—	1.5	1.5	>32	2	0.38	1.5	0.5	VSSA
$\Delta$ IIP-m	—	E146K	—	—	—	—	1	1	0.004	5	0.5	0.19	1	VSSA
$\Delta$ IIP-mr	—	E146K	—	H481Y	—	—	1	1	>32	3	0.5	0.5	0.75	VSSA
$\Delta$ IIP1 derivatives carrying <i>vraS</i> (S329L)														
$\Delta$ IIP1-g	S329L	—	N197S	—	—	—	3	6	0.006	>256	>32	2.5	0.75	hVISA
$\Delta$ IIP1-r	S329L	—	—	H481Y	—	—	3	12	>32	>256	>32	2	0.38	hVISA
$\Delta$ IIP1-gr	S329L	—	N197S	H481Y	—	—	3	6	>32	256	32	1.5	0.38	hVISA
$\Delta$ IIP2	S329L	E146K	—	—	—	—	3	12	0.004	>256	>32	2	0.5	hVISA
$\Delta$ IIP2 derivatives carrying both <i>vraS</i> (S329L) and <i>msrR</i> (E146K)														
$\Delta$ IIP2-r	S329L	E146K	—	H481Y	—	—	6	18	>32	>256	>32	2	0.38	VISA
$\Delta$ IIP3	S329L	E146K	N197S	—	—	—	4	12	0.003	192	>32	2	0.5	VISA
$\Delta$ IIP4	S329L	E146K	N197S	H481Y	—	—	12	12	>32	>256	>32	4	0.38	VISA
$\Delta$ IIP4-s	S329L	E146K	N197S	H481Y	—	$\Delta$ 67aa <sup>e</sup>	12	16	>32	>256	>32	4	0.38	VISA
$\Delta$ IIP5	S329L	E146K	N197S	H481Y	A297V	—	12	16	>32	256	>32	4	0.38	VISA
$\Delta$ IIP6	S329L	E146K	N197S	H481Y	A297V	$\Delta$ 67aa	12	12	>32	>256	>32	4	0.38	VISA

<sup>a</sup> Abbreviations: m, *msrR*(E146K); g, *graR*(N197S); r, *rpoB*(H481Y); s *sle1*( $\Delta$ 67aa).

<sup>b</sup> The position of the amino acid substitution in each gene is indicated. —, wild type (no mutation).

<sup>c</sup> Abbreviations: VAN, vancomycin; TEC, teicoplanin; RIF, rifampin; OXA, oxacillin; IPM, imipenem; DAP, daptomycin; LZD, linezolid.

<sup>d</sup> VAN phenotype, category of vancomycin susceptibility: VSSA, vancomycin MIC of <2 mg/liter; VISA, vancomycin MIC of 4 or 8 mg/liter; hVISA, vancomycin susceptibility judged by the shape of the population curve (Fig. 1).

<sup>e</sup> A sequence of 67 amino acids of *Sle1* was deleted from Mu50.

comparable to Mu50 (16, 17). Therefore, we expected that consecutive incorporation of three mutations, *vraS*(S329L), *graR*(N197S), and *rpoB*(H481Y), would convert  $\Delta$ IIP into a VISA strain. Unfortunately, the vancomycin MICs for the resultant  $\Delta$ IIP1 derivatives carrying *vraS*(S329L), *graR*(N197S), and *rpoB*(H481Y) ( $\Delta$ IIP1-gr,  $\Delta$ IIP1-g, and  $\Delta$ IIP1-r, respectively) were not the same as the vancomycin MIC of Mu50 (Table 2).

**Introduction of *msrR*(E146K) into  $\Delta$ IIP1 converted it to the VISA phenotype with a vancomycin MIC of 4  $\mu$ g/ml.** We recollected ourselves and looked for other candidate single nucleotide polymorphisms (SNPs) between VSSA strain  $\Delta$ IIP and hVISA strain Mu3. We inferred the presence of another mutation contributing to the increase in vancomycin resistance since there was a substantial difference in the vancomycin MICs for Mu3 (MIC = 3  $\mu$ g/ml) and  $\Delta$ IIP (MIC = 1  $\mu$ g/ml) (Table 2). The criteria for the candidate mutations were that they had to be (i) absent from the

N315 genome (which has the same chromosome as  $\Delta$ IIP except for a *meclI* deletion) (23) and (ii) shared by both Mu3 and Mu50. However, there were at least 174 SNPs between N315 and Mu50 (15, 19). Therefore, we first looked for the genes in Mu50 which we have identified to be capable of increasing the level of vancomycin resistance when expressed in excess in N315 (30). Among the 17 genes identified, we noticed that *msrR*(E146K) was present in Mu3 and Mu50 but that wild-type *msrR* was present in N315.

First, the increase in the vancomycin MIC was not seen in the  $\Delta$ IIP-derived mutants carrying wild-type *vraS* (Table 2). Therefore, the *vraS* mutation was considered an essential genetic event leading to acquisition of the VISA phenotype of Mu50, and without which mutation of the *msrR*, *graR*, or *rpoB* gene or combinations of these genes was not effective in raising the level of vancomycin resistance equivalent to that in Mu50 (Table 2). The first-step mutation *vraS*(I5N) or *vraS*(S329L) converted  $\Delta$ IIP

TABLE 3 Synthetic oligonucleotide primers

Plasmid constructed and primer designation	Sequence <sup>a</sup> (5'-3')	Gene <sup>b</sup>
pKOR1- <i>graR</i> (N197S)		
attB1- <i>graR</i> -FW	<u>GGGGACAAGTTTGTACAAAAAAGCAGGCTGTATTGAAGATTTTCGGCAAAGTAATGGATACA</u>	<i>sav0659</i>
attB2- <i>graR</i> -RV	<u>GGGGACCACTTTGTACAAAGAAAGCTGGGTATAATCAACTGTATGACGTT</u>	<i>sav0659</i>
pKOR1- <i>msrR</i> (E146K)		
attB1- <i>msrR</i> -FW	<u>GGGGACAAGTTTGTACAAAAAAGCAGGCTACAAGGTGGACAATCAAGAACAGATTCTATCATGGTTGTTC</u>	<i>sav1362</i>
attB2- <i>msrR</i> -RV	<u>GGGGACCACTTTGTACAAAGAAAGCTGGGTTCGTCATGTAAAATTATTAGAAGGTCGTTCCGGATGAACAAT</u>	<i>sav1362</i>
pKOR1- $\Delta$ <i>sle1</i>		
attB1- $\Delta$ <i>sle1</i> -FW	<u>GGGGACAAGTTTGTACAAAAAAGCAGGCTAGTAATTGCAGCTATTATTGGGACAAGCGCGATTAGCGCTGTTGCGGCA</u>	<i>sav0465</i>
attB2- $\Delta$ <i>sle1</i> -RV	<u>GGGGACCACTTTGTACAAAGAAAGCTGGGTAGTTTAGGATTCAATCCAACTTTCAGCTTGTGAAATGTA</u>	<i>sav0465</i>

<sup>a</sup> Underlining indicates *att* sequences introduced into the primer.

<sup>b</sup> The genes listed are specific for the chromosome of strain Mu50 (GenBank accession no. AP003367).

(vancomycin MIC = 1  $\mu$ g/ml) into pre-hVISA strain  $\Delta$ IP1 for which the vancomycin MIC was 2  $\mu$ g/ml. When *msrR*(E146K) was introduced as the second mutation, the phenotype of strain  $\Delta$ IP2 was converted to the hVISA phenotype and the vancomycin MIC was increased to 3  $\mu$ g/ml (Table 2). The shape of the curve for the  $\Delta$ IP2 population was equivalent to that for Mu3 (Fig. 1). Second, when the population analysis for vancomycin susceptibility between the *msrR*(E146K) mutant and its parent strain with wild-type *msrR* were compared, the three *msrR*(E146K) mutants  $\Delta$ IP2-r,  $\Delta$ IP3, and  $\Delta$ IP4 shifted to the right (Fig. 2A to C). In contrast, the oxacillin MICs for  $\Delta$ *msrR* mutants  $\Delta$ IP  $\Delta$ *msrR* and  $\Delta$ IP2 decreased (Table 2). Thus, these findings indicate that *msrR*(E146K) and *vraS*(S329L) led to increased resistance to vancomycin to a level similar to that in Mu3.

The vancomycin MIC for quadruple mutant  $\Delta$ IP4 was 12  $\mu$ g/ml, which corresponded to the MIC for VISA strain Mu50 (Table 2).  $\Delta$ IP4 also exhibited a population curve similar to that of Mu50 (Fig. 1). Therefore, the introduction of four mutated genes, *vraS*, *msrR*, *graR*, and *rpoB*, into a VSSA strain reconstituted the VISA phenotype.

**Cell wall thickening of  $\Delta$ IP4 is an inducible phenotype.** We

consider cell wall thickening to be a cardinal feature of the VISA phenotype that is directly associated with the clogging mechanism of vancomycin resistance (2, 36). As shown in Table 4, the *vraS*(S329L) mutation thickened the cell wall of  $\Delta$ IP so that the thickness of its cell was comparable to that of the cell wall of clinical hVISA strain Mu3.  $\Delta$ IP2 carrying both the *msrR*(E146K) and *vraS*(S329L) mutations showed a thickened cell wall (34.7 nm); however, VISA strain Mu50 had a much thicker cell wall (38.5 nm) (Table 4).

We expected our  $\Delta$ IP4 construct to have a cell wall as thick as that of Mu50. Contrary to our expectation, however, the thickness of the cell wall of  $\Delta$ IP4 was only 31.6 nm, which was almost the same as that of the cell wall of  $\Delta$ IP1 (30.8 nm) and hVISA strain Mu3 (28.7 nm) (Table 4). To reconcile the contradictory observations of vancomycin resistance and a thin cell wall, we considered the possibility of the induction of thickening of the cell wall of  $\Delta$ IP4. The cell wall of  $\Delta$ IP4 increased from 31.6 to 35.8 nm after 10 min of exposure to 10  $\mu$ g/ml of vancomycin. This cell wall thickness corresponded to the cell wall thickness (38.5 nm) of Mu50 exposed to vancomycin. Curiously,  $\Delta$ IP4 was the only strain tested whose cell wall increased in thickness. The thickness of the cell

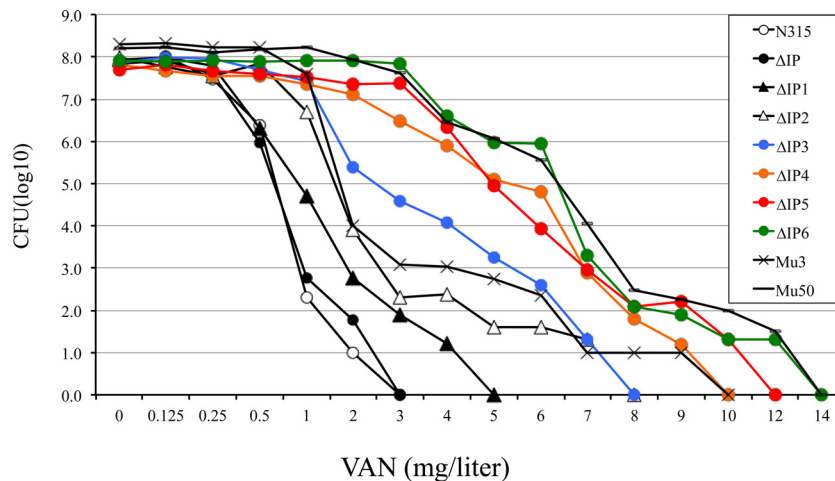


FIG 1 Population analysis of the susceptibility profiles of the vancomycin (VAN)-resistant subpopulation. The profiles of  $\Delta$ IP, its derivatives, Mu3, and Mu50 were evaluated after 72 h of incubation at 37°C. The sequential introduction of six mutations, resulting in strains  $\Delta$ IP1,  $\Delta$ IP2,  $\Delta$ IP3,  $\Delta$ IP4,  $\Delta$ IP5, and  $\Delta$ IP6, reconstituted the VISA phenotype of Mu50 in VSSA strain N315 $\Delta$ IP. About  $10^7$  CFU of the overnight culture of each strain was inoculated on BHI agar plates containing various concentrations of vancomycin.

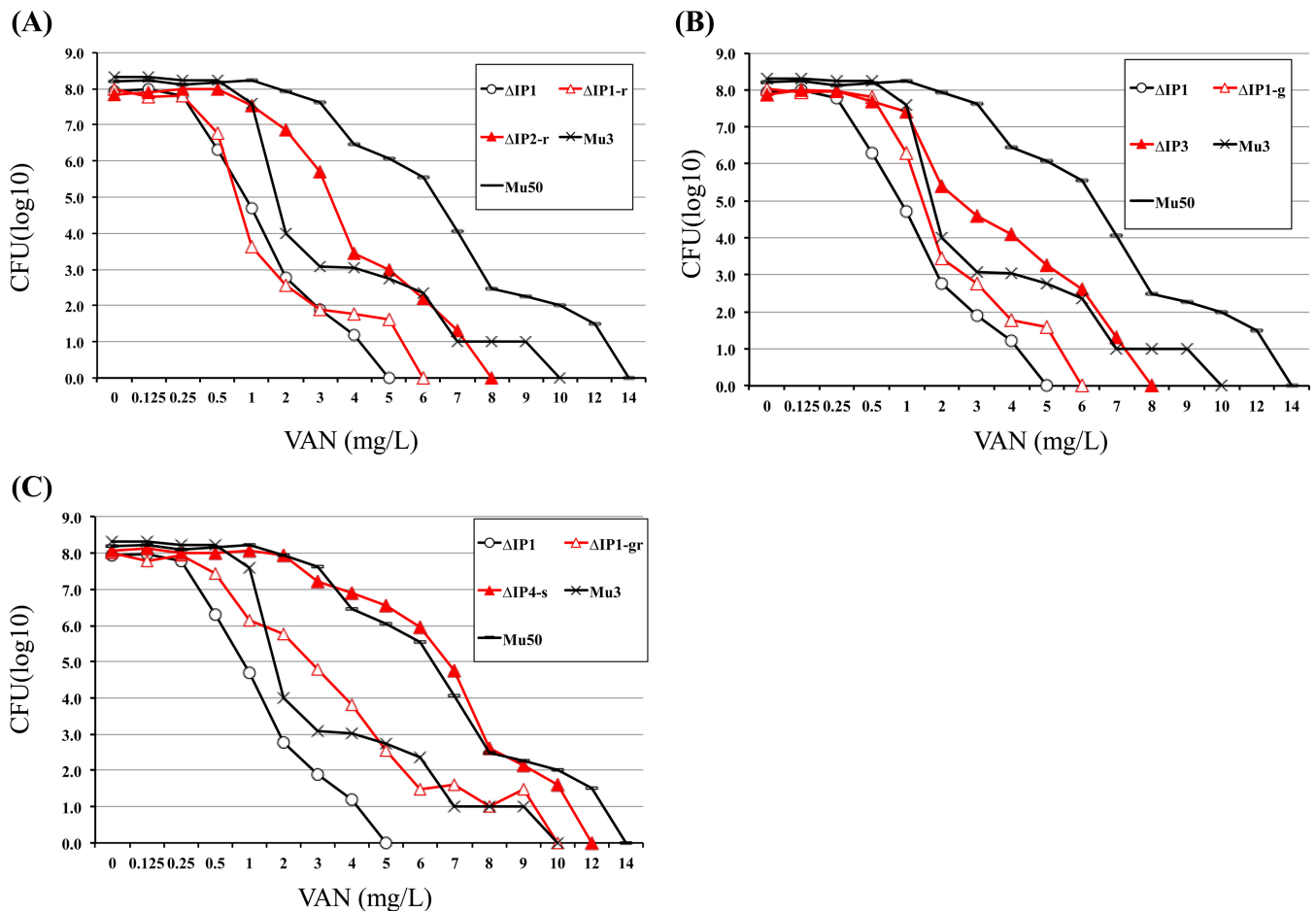


FIG 2 The *msrR*(E146K) mutation confers increasing resistance to vancomycin. The profiles of the resistant subpopulations of strain  $\Delta$ IP, its derivative mutants, hVISA Mu3, and VISA Mu50 are shown. The number of cells (in  $\log_{10}$  CFU per milliliter) growing on BHI agar containing vancomycin are shown on the y axis. Vancomycin concentrations are shown on the x axis. The number of the colonies that grew was counted after incubation at 37°C for 48 h. Red open triangles and red closed triangles, the strain with wild-type *msrR* and the *msrR*(E146K) mutant, respectively.

walls of the other strains, including Mu50, decreased in response to vancomycin. However, clinical VISA strains, including Mu50, have a constitutively thickened cell wall. Therefore, we looked for another mutation in Mu50 that was responsible for the constitutive increase in cell wall thickness. There are nine nonsynonymous SNPs between Mu3 and Mu50 (3). *fdh2*(A297V) (*fdh2* is the ortholog of *sa2102* of N315), encoding a putative mutated formate dehydrogenase (Fdh), was among these SNPs. We designated the mutated gene *fdh2*, since another *fdh* gene presumably encodes Fdh in Mu50 (6). Another candidate SNP is *sle1*, encoding *N*-acetylmuramoyl-*l*-alanine amidase. A deletion of 67 amino acids ( $\Delta$ 67aa) from the *lysM* domain was found in the *sle1* gene of Mu50 (3). *Sle1* attachment to the cross wall is abolished in staphylococcal *tagO* mutants, which are defective for WTA synthesis (27, 28). We introduced the *sle1*( $\Delta$ 64aa) or *fdh2*(A297V) gene into  $\Delta$ IP4 or  $\Delta$ IP5 and then obtained strain  $\Delta$ IP4-s or  $\Delta$ IP6 to test the effects of the genes on cell wall thickness, respectively. The vancomycin MIC did not change, nor did the MICs of the other antibiotics (Table 2 and Fig. 1). However, significant cell wall thickening was observed in  $\Delta$ IP4-s and  $\Delta$ IP6 (cell wall thicknesses, 40.9 nm and 39.7 nm, respectively) compared to the cell wall thicknesses of their parent strains,  $\Delta$ IP4 and  $\Delta$ IP5, respectively (Table 4). The six

mutants of  $\Delta$ IP attained the VISA phenotype of Mu50 with a constitutive increased cell wall thickness (Fig. 3).

**Progressive decrease in growth rate and autolytic activity of the mutant strains which showed increased vancomycin resistance.** A low growth rate is a characteristic feature of strains with the VISA phenotype. Their growth curves showed a shift toward the right as the numbers of mutations increased. The calculated doubling time also increased with the increase in vancomycin resistance of the strains (Table 4). Among the six mutations, *rpoB*(H481Y) had a pronounced effect on slowing the growth of strains  $\Delta$ IP4,  $\Delta$ IP5, and  $\Delta$ IP6 (Table 4).

Figure 4 illustrates the results of the assay of autolysis in the presence of 0.05% Triton X-100. We compared the autolytic activity with the percent decrease in the OD<sub>660</sub> after 4 h of incubation shown in Table 4. A decrease in the rate of cell lysis was observed with the sequential introduction of mutations. When the autolysis activities of *msrR*(E146K) mutant  $\Delta$ IP2 and the  $\Delta$ IP1  $\Delta$ *msrR* strain were compared, the level of activity in  $\Delta$ IP2 decreased compared to that in its parent strain,  $\Delta$ IP1, but it was not changed in the  $\Delta$ IP1  $\Delta$ *msrR* mutant. This finding indicates that *msrR*(E146K) is associated with a decrease in autolytic activity. After 4 h, the  $\Delta$ IP2,  $\Delta$ IP4, and  $\Delta$ IP5 mutants showed a decrease in

TABLE 4 Prolonged doubling time, thickening of cell wall, and autolytic activity in  $\Delta$ IIP derivative strains

Strain <sup>a</sup>	Phenotype	Doubling time (min)	Autolysis (% decrease of OD) <sup>c</sup>	Cell wall thickness (nm)	
				Without vancomycin	With VAN10 <sup>c</sup>
Clinical isolates and control strains					
$\Delta$ IIP	VSSA	26.2	68.1	19.4 $\pm$ 2.9	18.5 $\pm$ 1.3
$\Delta$ IIP1	hVISA	28.3	51.1	30.8 $\pm$ 4.3	23.7 $\pm$ 2.1
Mu3	hVISA	35.7 <sup>b</sup>	55.5	28.7 $\pm$ 3.2	25.7 $\pm$ 1.8
Mu50	VISA	37.1 <sup>b</sup>	26.9	38.5 $\pm$ 4.8 <sup>d</sup>	36.0 $\pm$ 1.8 <sup>d</sup>
$\Delta$ IIP-derived mutants					
$\Delta$ IIP-m	VSSA	29.8	NT <sup>g</sup>	17.5 $\pm$ 1.0	NT
$\Delta$ IIP-g	VSSA	30.5	NT	NT	NT
$\Delta$ IIP-r	VSSA	29.7	NT	NT	NT
$\Delta$ IIP-gr	VSSA	30.3	NT	NT	NT
$\Delta$ IIP-mr	VSSA	30.6	NT	NT	NT
$\Delta$ IIP1-derived mutants					
$\Delta$ IIP1-g	hVISA	28.0	NT	26.7 $\pm$ 2.4	NT
$\Delta$ IIP1-r	hVISA	29.5	NT	25.1 $\pm$ 1.6	NT
$\Delta$ IIP2	hVISA	27.6	21.2	34.7 $\pm$ 4.4 <sup>d</sup>	30.8 $\pm$ 3.6
$\Delta$ IIP1 $\Delta$ msrR	VSSA	31.4	36.1	Unmeasurable <sup>f</sup>	Unmeasurable
$\Delta$ IIP2-derived mutants					
$\Delta$ IIP3	VISA	27.8	57.3	32.8 $\pm$ 3.8	28.7 $\pm$ 4.1
$\Delta$ IIP4	VISA	37.4 <sup>b</sup>	0.15	31.6 $\pm$ 3.3	35.8 $\pm$ 2.0 <sup>d</sup>
$\Delta$ IIP4-s	VISA	35.0	0.3	40.9 $\pm$ 3.6 <sup>d</sup>	41.5 $\pm$ 2.9 <sup>d</sup>
$\Delta$ IIP5	VISA	36.3 <sup>b</sup>	0.7	36.7 $\pm$ 3.2 <sup>d</sup>	33.0 $\pm$ 2.8 <sup>d</sup>
$\Delta$ IIP6	VISA	37.6 <sup>b</sup>	27.9	39.7 $\pm$ 4.5 <sup>d</sup>	46.1 $\pm$ 4.8 <sup>d</sup>

<sup>a</sup> Abbreviations: m, *msrR*(E146K); g, *graR*(N197S); r, *rpoB*(H481Y); s, *sle1*( $\Delta$ 67aa).

<sup>b</sup>  $P < 0.001$  for the difference in doubling time from that for  $\Delta$ IIP.

<sup>c</sup> Triton X-100-induced autolysis of the representative strain. The data represent the percent decrease in the OD<sub>660</sub> after 4 h of incubation.

<sup>d</sup>  $P < 0.001$  for the difference in length from that for  $\Delta$ IIP1 (previously designated strain  $\Delta$ IIP-H14).

<sup>e</sup> The thickness of the cell wall was measured after induction with vancomycin at 10  $\mu$ g/ml (VAN10) for 10 min.

<sup>f</sup> The photograph taken by transmission electron microscopy is shown in Fig. 6.

<sup>g</sup> NT, not tested.

autolytic activity; however, the autolytic activity in  $\Delta$ IIP6 was similar to that in Mu50 (Table 4).

**Effects of *msrR*(E146K),  $\Delta$ msrR, and *sle1*( $\Delta$ 64aa) on morphology and cell separation phenotypes.** To investigate the effects of the *msrR*(E146K) and *sle1*( $\Delta$ 64aa) genes on phenotypic expression, we constructed three mutant strains,  $\Delta$ IIP  $\Delta$ msrR,  $\Delta$ IIP1  $\Delta$ msrR and  $\Delta$ IIP4-s, and then compared their phenotypes to those of strains  $\Delta$ IIP1,  $\Delta$ IIP2, and  $\Delta$ IIP5. In the absence of vancomycin, overnight cultures of the  $\Delta$ IIP  $\Delta$ msrR,  $\Delta$ IIP1  $\Delta$ msrR, and  $\Delta$ IIP4-s mutant strains aggregated (see Fig. S1 in the supplemental material). When analyzed by transmission electron microscopy, those cells failed to separate and showed an abnormal morphology. In contrast, the culture and cells of  $\Delta$ IIP2,  $\Delta$ IIP5, and their parent strains,  $\Delta$ IIP and  $\Delta$ IIP4, respectively, showed a normal morphology. Interestingly,  $\Delta$ IIP5, carrying both the *msrR*(E146K) and *sle1*( $\Delta$ 64aa) mutations, showed increased resistance to vancomycin and reduced autolytic activity and maintained normal separation and a normal morphology. This finding indicates that the *fdh*(A297V) mutation allowed the abnormal separation caused by *sle1*( $\Delta$ 64aa) in  $\Delta$ IIP5 to be recovered.

**Effects of increasing vancomycin resistance on the relationship between mutated *rpoB* and three mutated genes, *vraS*, *msrR*, and *graR*.** The *rpoB*(H481Y) mutation was also related to the three phenotypes of increasing resistance to vancomycin (Table 2), slow growth (Table 4), and decreased autolytic activity (Fig. 4), as we have reported previously (17). However, the effects

of increasing vancomycin resistance on the interaction between *rpoB*(H481Y) and the other three mutated genes, *vraS*(S329L), *msrR*(E146K), and *graR*(N197S), are unknown. To clarify the interaction, we investigated the rate of appearance of hVISA or VISA among the *rpoB*(H481Y) mutants when the  $\Delta$ IIP and  $\Delta$ IIP1 mutants were selected by rifampin. We isolated 20 rifampin-resistant isolates carrying the *rpoB* mutation from each of six mutants,  $\Delta$ IIP-m,  $\Delta$ IIP-g,  $\Delta$ IIP1,  $\Delta$ IIP2,  $\Delta$ IIP1-g, and  $\Delta$ IIP3, and parent strain  $\Delta$ IIP and then determined the MIC of vancomycin by the Etest (Table 5). Interestingly, each of the 20 *rpoB* mutant strains showed a variety of MICs. For 2 (10%), 3 (15%), 20 (100%), 1 (5%), 11 (55%), 3 (15%), and 12 (60%) of 20 of the *rpoB* mutant isolates of  $\Delta$ IIP,  $\Delta$ IIP-m,  $\Delta$ IIP-g,  $\Delta$ IIP1,  $\Delta$ IIP2,  $\Delta$ IIP1-g, and  $\Delta$ IIP3, respectively, the vancomycin MIC was increased compared to that for the parent strain. Among these isolates, 11 (55%) and 3 (15%) of the *rpoB* mutants of hVISA strains  $\Delta$ IIP2 and  $\Delta$ IIP1-g, respectively, changed to VISA (vancomycin MIC  $\geq$  4  $\mu$ g/ml). In particular, 3 (15%) *rpoB* mutants of  $\Delta$ IIP3 showed phenotypic expression of Mu50-like VISA resistance (vancomycin MIC = 8  $\mu$ g/ml). Therefore, it was revealed that a genetic background of all three mutations in *vraS*, *msrR*, and *graR* was needed for conversion of Mu50-like VISA phenotype induced by mutated *rpoB*.

**Transcriptional profiles of genes related to peptidoglycan and WTA synthesis among  $\Delta$ IIP-derived strains and control strains.** The transcriptional profiles of the  $\Delta$ IIP-derived strains were analyzed (GEO accession no. GSE43643). The levels of the

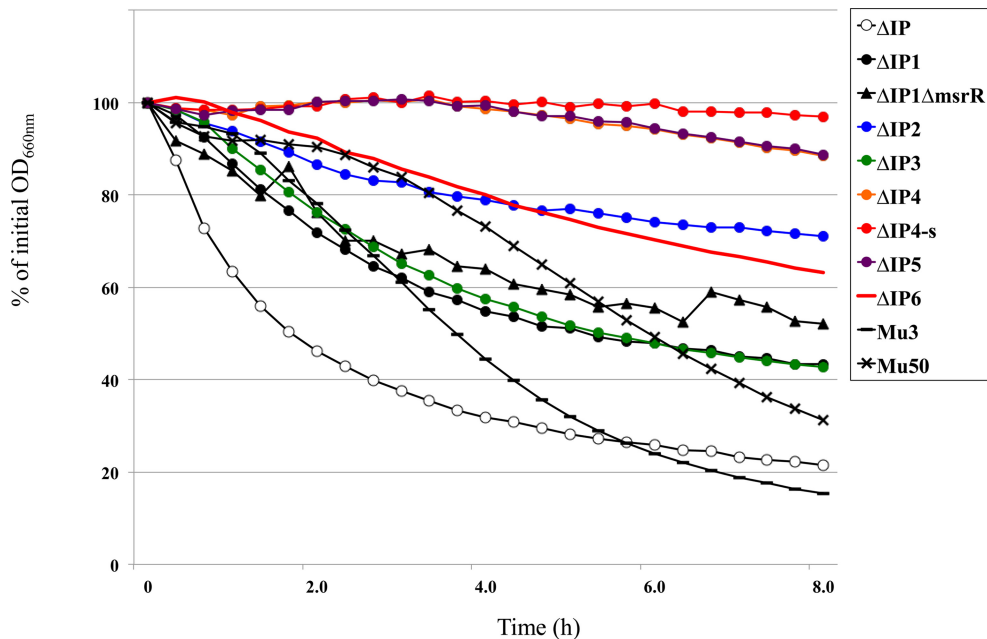


**FIG 3** Reduction of autolytic activity in  $\Delta$ IP mutant strains. The Triton X-100-stimulated autolysis of the parental strain ( $\Delta$ IP), its derivatives, hVISA Mu3, and Mu50 is shown. Cultures were suspended in autolysis buffer to an initial  $OD_{660}$  of 2.0, and the rates of autolysis were monitored as the decrease in  $OD_{660}$  with time. The activities of strains  $\Delta$ IP2,  $\Delta$ IP4,  $\Delta$ IP4-s, and  $\Delta$ IP5 were decreased compared with those of the parent strains, other mutants, hVISA Mu3, and VISA Mu50. Autolysis was measured as the decline in the optical density versus time and is expressed as the percentage of the initial optical density. The percent decrease in  $OD_{660}$  after 4 h of incubation is shown in [Table 4](#).

transcripts of 51 genes encoding peptidoglycan and WTA synthesis and the 6 genes *vraSR*, *msrR*, *graR*, *rpoB*, *fdh2*, and *sle1* in mutant strain  $\Delta$ IP1 were compared to those in  $\Delta$ IP (see Fig. S2 and S3 in the supplemental material). Of the 51 genes encoding peptidoglycan and WTA synthesis, 10 genes were upregulated by the presence of the *vraS*(S329L) mutation (see Fig. S2 in the supplemental material). Of these 10 upregulated genes, the *vraSR*, *msrR*(E146K), and *murZ* (encoding UDP-*N*-acetylglucosamine 1-carboxyvinyltransferase) genes were upregulated in the  $\Delta$ IP2,  $\Delta$ IP3, and  $\Delta$ IP4 *msrR*(E146K) mutants compared to their levels of transcription in the strain with wild-type *msrR*. However, the other 9 genes associated with the cell wall synthesis stimulon were downregulated (see Fig. S2A in the supplemental material). The data indicate that the *msrR* mutation allowed the recovery of the level of transcription of several genes that were up- or downregulated by the *vraS* mutation.

In contrast, the transcriptional profiles of the  $\Delta$ IP5 strain were different from those of the other strain  $\Delta$ IP-derived strains. The levels of transcription of *fdh2*(A297V), *vraS*(S329L), *vraR*, *murF*, *murZ*, *murG*, *murQ*, SA0511, SAA0522, and *capG* genes increased by greater than 2-fold in  $\Delta$ IP5 compared to their levels of transcription in  $\Delta$ IP (see Fig. S2A in the supplemental material). The *murZ*, *murQ* (encoding *N*-acetylmuramic acid 6-phosphate esterase), *sa0523* [encoding poly(glycerol-phosphate)  $\alpha$ -glucosyltransferase], *sa0524* (encoding GTP cyclohydrolase), *sa0511* (encoding GDP-mannose 4,6-dehydratase), and *capG* (encoding the capsular polysaccharide synthesis protein Cap5G) genes were upregulated in  $\Delta$ IP5, and upregulation of these genes is common to Mu50 (see Fig. S2A and S3A in the supplemental material). The transcriptional profiles of  $\Delta$ IP5 were not similar to those of the other  $\Delta$ IP-derived strains, hVISA strain Mu3, and slow VISA

strain  $\Delta$ IP *rpoB*(R512P), except for the upregulation of the *vraSR* and *murZ* genes (19).

**Transcriptional profiles of 19 genes related to the pyrimidine metabolic pathway.** During the course of the study, the downregulation of numerous members of the pyrimidine operon, comprising *pyrAB*, *pyrB*, *pyrC*, *pyrE*, *pyrF*, *pyrG*, and *pyrH*, as well as that of the regulator *pyrR*, was detected in  $\Delta$ IP4,  $\Delta$ IP5, and Mu50 carrying *rpoB*(H481Y) (see Fig. S2B and S3B in the supplemental material).

Moreover, the *cmk* gene, encoding cytidylate kinase, was downregulated in strains  $\Delta$ IP5 and Mu50. It has been reported that the reduced cytidylate kinase activity in *cmk* mutant strains contributes to the conversion from the hVISA phenotype to the VISA phenotype by thickening the cell wall and reducing the cell growth rate (6). It was indicated that the *pyr* operon and *cmk* were downregulated and the *ndk* gene (encoding nucleoside diphosphate kinase) was upregulated by the presence of *fdh2*(A297V) (see Fig. S2B in the supplemental material).

**Transcriptional profiles of 27 genes related to the pathway from pentose phosphate to cell wall synthesis by way of glycolysis.** To investigate why an increase in the thickness of the cell wall of the  $\Delta$ IP4 mutant strain was induced by vancomycin, the transcriptional profiles of cells in cultures with and without vancomycin were compared. In the  $\Delta$ IP1 strain, the *glmS*, *sa0529*, and *sa0528* genes, which are associated with the metabolic pathway from D-ribulose-5-phosphate (pentose phosphate pathway) to glucosamine-6-phosphate (GlcN6P) by way of D-fructose-6-phosphate (glycolysis), were upregulated (see Fig. S2C and S3C in the supplemental material). In addition, the *sa2127* (encoding ribose-5-phosphate isomerase A), *fbp*-like (encoding fructose-bisphosphatase), *gnd* (encoding 6-phosphogluconate dehydroge-

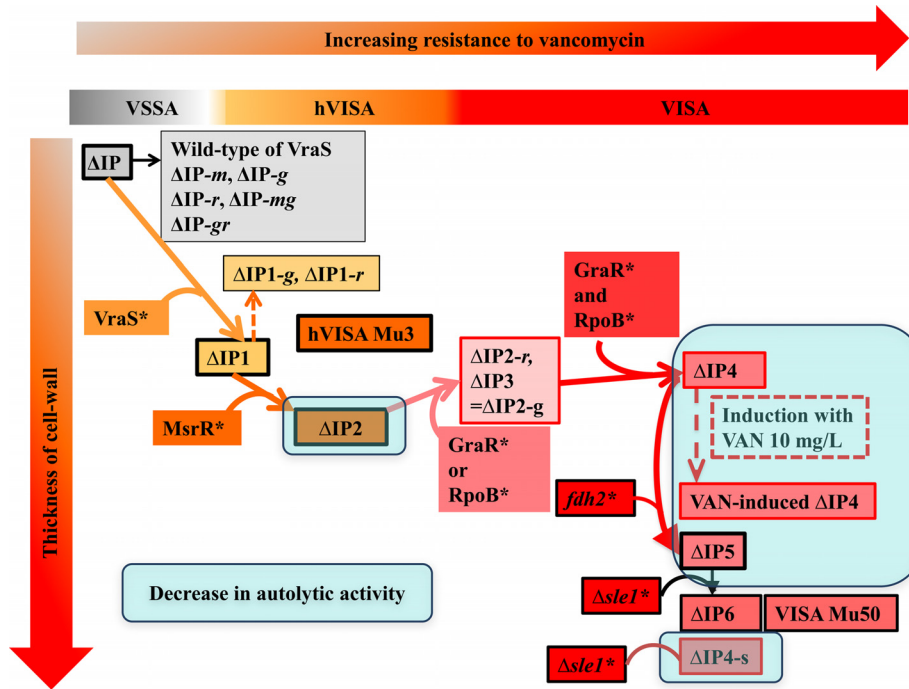


FIG 4 Steps in which phenotypic Mu50-like VISA is reconstituted from VSSA parent strain  $\Delta$ IP. The increase in resistance to vancomycin was related to the two phenotypes' cell wall thickness and autolytic activity among the  $\Delta$ IP isogenic laboratory strains. The cell wall thickness is shown on the y axis. The level of vancomycin resistance is shown on the x axis. The blue areas describe a mutant strain with decreased autolytic activity.

nase), and *pgi* (encoding glucose-6-phosphate isomerase) genes were downregulated in  $\Delta$ IP1, as shown in Fig. S2C in the supplemental material. Interestingly, in  $\Delta$ IP2,  $\Delta$ IP3, and  $\Delta$ IP4, carrying the *msrR*(E146K) mutation, the levels of transcripts of the *glmS* gene increased. Contrary to expectations, the *gntP* (encoding gluconate permease), *gntK* (encoding glucokinase), *gntR* (encoding the gluconate operon transcriptional repressor), and *fbp* genes were upregulated in  $\Delta$ IP5 and Mu50 but not in Mu3 or the other  $\Delta$ IP-derived strains. The profiles in slow VISA strain  $\Delta$ IP *rpoB*(R512P) were also different from those in the other strains (see Fig. S2C and S3C in the supplemental material).

Comparison of the differences in the transcriptional profiles between strains induced with vancomycin and strains not induced with vancomycin showed that the levels of transcripts of the *gntR* and *gntK* genes increased in  $\Delta$ IP4 induced with vancomycin but not in  $\Delta$ IP4 not induced with vancomycin (see Fig. S2B and S3C in

the supplemental material). The transcriptional profile in  $\Delta$ IP4 induced with vancomycin was similar to that in  $\Delta$ IP5 and Mu50.

DISCUSSION

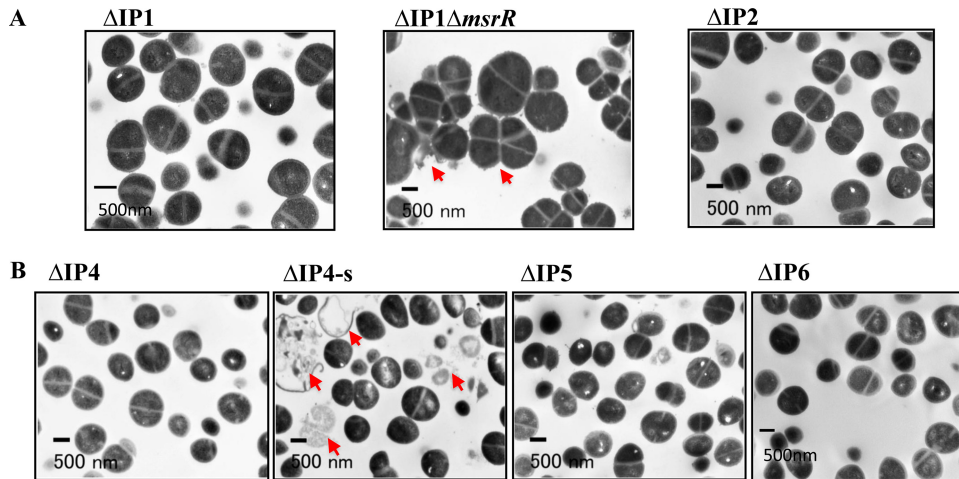
The VISA phenotype of Mu50 was successfully reconstituted in VSSA strain N315 $\Delta$ IP by the sequential introduction of six mutations, i.e., *vraS*(S329L), *msrR*(E146K), *graR*(N197S), *rpoB*(H481Y), *fdh2*(A297V), and *sle1*( $\Delta$ 67aa). Our study had six major findings. First, we proved the stepwise increase in phenotypic resistance from VSSA strain  $\Delta$ IP to Mu50-like VISA, by way of hVISA, using an isogenic library. This finding supports the hypothesis that gene mutations led by pressure from antibiotic therapy of MRSA infections constructed a phenotypic VISA strain from a MRSA (VSSA) strain in a hospital. In practical terms, we also revealed that exposure not only to vancomycin but also to

TABLE 5 Distribution of amino acid substitutions in *rpoB* among  $\Delta$ IP mutants by selection with rifampin

Strain <sup>a</sup>	Vancomycin MIC (mg/liter)	No. of mutants selected with rifampin with the following mutation in <i>rpoB</i> <sup>b</sup> :										Total
		Q468K	Q468L	Q468R	D471V	N474K	A477D	H481R	H481Y	R484H	S486L	
$\Delta$ IP	1	0	0	1 (1, 0, 0)	0	0	0	0	8 (3, 3, 2)	2 (0, 2, 0)	9 (0, 9, 0)	20 (4, 14, 2)
$\Delta$ IP-m	1	0	0	0	0	3 (0, 2, 1)	0	0	2 (0, 1, 1)	2 (0, 1, 1)	13 (1, 12, 0)	20 (1, 16, 3)
$\Delta$ IP-g	1	0	0	0	0	0	0	0	5 (0, 0, 5)	0	15 (0, 0, 15)	20 (0, 0, 20)
$\Delta$ IP1	2	12 (7, 5, 0)	0	0	0	0	0	0	7 (5, 1, 1)	0	1 (0, 1, 0)	20 (12, 7, 1)
$\Delta$ IP2	3	3 (2, 1, 0)	0	0	0	0	0	0	8 (0, 2, 6)	0	9 (0, 4, 5)	20 (2, 7, 11)
$\Delta$ IP1-g	3	1 (0, 0, 1)	0	0	1 (0, 1, 0)	0	3 (0, 2, 1)	0	1 (0, 1, 0)	0	14 (3, 10, 1)	20 (3, 14, 3)
$\Delta$ IP3	4	0	6 (0, 2, 4)	0	1 (0, 1, 0)	0	1 (0, 0, 1)	1 (0, 0, 1)	6 (0, 1, 5)	0	5 (0, 4, 1)	20 (0, 8, 12)
Total		16 (9, 6, 1)	6 (0, 2, 4)	1 (1, 0, 0)	2 (0, 2, 0)	3 (0, 2, 1)	4 (0, 2, 2)	1 (0, 0, 1)	37 (8, 9, 20)	4 (0, 3, 1)	66 (4, 40, 22)	140 (22, 66, 52)

<sup>a</sup> Abbreviations: m, *msrR*(E146K); g, *graR*(N197S).

<sup>b</sup> Selection was with rifampin at 1  $\mu$ g/ml. Data are for 20 mutants of each strain. The three values in parentheses are the numbers of mutants with vancomycin MICs that were decreased, invariant, or increased, respectively, compared with the vancomycin MIC for the parent strain.



**FIG 5** Abnormal morphology of the  $\Delta IP1 \Delta msrR$  and  $\Delta IP4-s$  mutant strains in the absence of vancomycin. Cells were analyzed by transmission electron microscopy. All strains were grown from small inocula under the same standard conditions in BHI medium free of vancomycin. The morphology of the cells in the bacterial cultures was observed by phase-contrast microscopy, and the cells were also analyzed by transmission electron microscopy. In comparison with the morphology of the parental strain, the cultures of  $\Delta IP1$ ,  $\Delta IP2$ ,  $\Delta IP4$ , and  $\Delta IP5$  were composed of regularly shaped and well-separated cocci, and cultures of the  $\Delta IP1 \Delta msrR$  and  $\Delta IP4-s$  strains grew as multicellular aggregates. Electron microscopic sections of  $\Delta IP1 \Delta msrR$  and  $\Delta IP4-s$  show clusters of unseparated cells with abnormally thick cell walls, and the cells are also surrounded by a large amount of amorphous extracellular material (red arrows). However, cells of the *msrR*(E146K) mutant strain are normally shaped.  $\Delta sle1$  mutant strain  $\Delta IP4-s$  failed to separate and had a much thicker cell wall than Mu50, although the cell walls of  $\Delta IP5$  and  $\Delta IP6$  showed a normal separation that was the same as that of Mu50.

imipenem and rifampin selected for hVISA strains carrying *vraS*(S329L) in this study (10).

Second, the results shown in Table 2 indicate that naive *vraS* mutants ( $\Delta IP$  derivatives) and naive *msrR* mutants ( $\Delta IP1$  derivatives) did not convert to phenotypic VISA or hVISA from VSSA. In contrast, mutants with both *vraS*(S329L) and *msrR*(E146K) had a tendency to convert to an hVISA phenotype similar to that of hVISA strain Mu3. When mutants with both *vraS*(S329L) and *msrR*(E146K) were selected by rifampin (Table 5), the level of vancomycin resistance increased, which was indicated by the high frequencies of vancomycin resistance in 11/20 (55%) and 12/20 (60%) isolates of the  $\Delta IP2$  and  $\Delta IP3$  mutants, respectively. It was suggested that both the *vraS*(S329L) and *msrR*(E146K) mutations are essential for conversion to phenotypic VISA by rifampin. As the *msrR*(E146K) or *vraS*(S329L) mutation was present in 19.4 and 15.8% of clinically isolated hVISA and VISA strains, respectively (11), clinicians should be aware of these findings before prescribing rifampin therapy.

Third, *msrR*(E146K) is responsible for conversion to the Mu3-type hVISA phenotype. *msrR* regulates genes encoding cell wall synthesis and antibiotic resistance: *hmrA*, *sarH*, *sigB*, etc. However, the data indicate that *msrR*(E146K) downregulated several genes related to cell wall and WTA synthesis (see Fig. S2A and S3A in the supplemental material). *msrR*, which is a member of the LytR-CspA-Psr (LCP) family of membrane proteins, contributes to the development of high-level resistance to  $\beta$ -lactam antibiotics (37) and cell surface characteristics and virulence in *S. aureus* (38, 39). In this study, we also demonstrated that the *msrR*(E146K) mutation influences resistance to  $\beta$ -lactams and glycopeptides (Table 2), as reported previously (7). The  $\Delta msrR$  mutation led to reduced resistance to oxacillin (Table 2), and the cells failed to separate fully and showed aberrant septal placement (Fig. 5). Chan et al. reported that a  $\Delta lcp$  mutant showed a defect in tethering WTA to the cell wall; cleaved WTA synthesis intermediates, releasing ribitol phosphate into the medium; and recycled bacto-

prenon for peptidoglycan synthesis (40). It has been reported that *lcp*, including *msrR* of *S. aureus*, encodes promiscuous enzymes that attach secondary cell wall polymers with discrete linkage units to peptidoglycan (40). Thus, it was suggested that the *msrR*(E146K) mutation promotes the tethering of WTA and the capsule to the cell wall, which then leads to decreased autolytic activity and resistance to vancomycin.

Fourth, the *rpoB*(H481Y) mutation was related not only to an increase in vancomycin resistance but also to a low growth rate and decreased autolysin activity (Fig. 4 and Table 4). The *rpoB*(H481Y) mutation was also previously related to an increase in resistance to vancomycin (10, 17, 21). For the subpopulation for which the vancomycin MIC was 4  $\mu\text{g}/\text{ml}$ , for example, for the  $\Delta IP1-r$  strain, the number of CFU was  $5 \times 10^2$ , which was similar to the value for hVISA strain Mu3. The *rpoB*(H481Y) mutation has been found in Mu50 and 70% of VISA strains throughout the world (41) and is related to the increase in the rates of resistance to vancomycin and daptomycin (10). Recently, we have also reported that the RNA polymerase mutation *rpoB*(R512P) acts on reversible resistance to vancomycin (19) and seems to have a regulatory effect in triggering the entire scheme of peptidoglycan synthesis. We have reported that the *rpoB* and *rpoC* mutations are regulatory mutations (17, 19, 42, 43). It was supposed that the *rpoB* mutation acts as a regulatory mutation in the acquisition of the VISA phenotype.

The *rpoB*(H481Y) mutants  $\Delta IP4$ ,  $\Delta IP5$ , and Mu50 showed significant downregulation of the *pyr* genes. The products of the *pyr* operon are involved in the *de novo* synthesis of pyrimidine nucleotides from bicarbonate and from intermediates of central carbon metabolism or via salvage of preformed pyrimidine bases and nucleotides present in the medium. The *pyr* operon is regulated by transcription attenuation in response to exogenous uracil, which was determined using transcription studies and determination of the intracellular pyrimidine triphosphate nucleoside, UDP, and UMP/phosphoribosyl pyrophosphate (PRPP) pool size (44). In

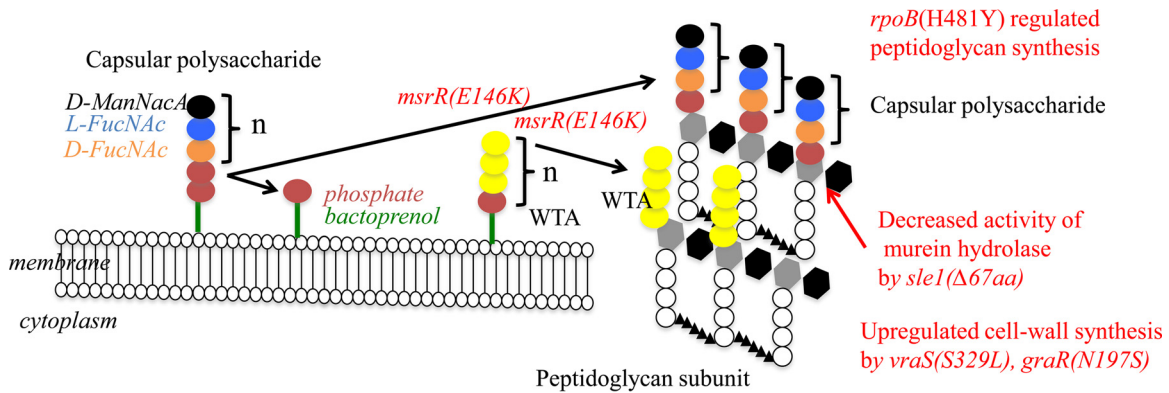


**FIG 6** Possible effect of mutations in six genes on Mu50-type vancomycin resistance. (i) In  $\Delta$ IP1, upregulated cell wall synthesis results in an increase in cell wall thickness. (ii) In  $\Delta$ IP2, autolytic activity is decreased, and because of the deposition of LysM-type murein hydrolase, the cell division type was restricted and tethering of WTA and capsular polysaccharide to the cells was increased. (iii) In  $\Delta$ IP3, upregulated cell wall synthesis results in an increase in cell wall thickness and conversion from the hVISA to VISA phenotype. (iv) In  $\Delta$ IP4, a regulatory mutation resulted in slow growth and an increase in cell wall thickness. (v) In  $\Delta$ IP5, resistance to vancomycin occurred with the presence of other mutated genes. The function is unknown. It seems that the *fdh2*(A297V) mutation regulates the moderate activity of the  $\Delta$ *sle1* mutant. (vi) In  $\Delta$ IP6, the activity of LysM-type murein hydrolase (autolysis) was decreased, resulting in an increase in cell wall thickness and resistance to vancomycin.

*Bacillus subtilis*, PyrR controls the expression of the *pyr* operon by binding to specific sequences of *pyr* mRNA, thereby leading to the attenuation of transcription (45, 46) in response to exogenous uracil and to intracellular PRPP pools (described below).

Moreover, it was found for the first time that vancomycin induced an increase in cell wall thickness in  $\Delta$ IP4. The thickening of the cell wall of  $\Delta$ IP4 was increased by induction with vancomycin at 10  $\mu$ g/ml, although the cell walls of  $\Delta$ IP5 and Mu50 were thickened constitutively.

Fifth, we verified the effects of the *msrR*(E146K) and *sle1*( $\Delta$ 67aa) mutations. The deposition of LysM murein hydrolases of *sle1* in the envelope of  $\Delta$ *lcp* mutant staphylococci was detected (Fig. 6). The decoration of staphylococcal peptidoglycan with WTA restricts the binding of secreted murein hydrolases to the cell wall and limits the autolytic activity of these enzymes on the cross-wall compartment of dividing staphylococci. These data suggest that the WTA deposition defect of the  $\Delta$ *lcp* mutant with the  $\Delta$ *msrR* mutation causes the unrestricted deposition of murein hydrolases in the bacterial envelope, a phenotype that likely contributes to the decreased viability of the  $\Delta$ *msrR* daughter cells generated during cell division.

Finally, several other genes involved in cell wall synthesis and modification were found to respond to vancomycin. *GlmS* activity has a critical role in the initiation of PG synthesis, which increased in the  $\Delta$ IP1,  $\Delta$ IP2,  $\Delta$ IP3, and  $\Delta$ IP4 strains without vancomycin. It has recently been reported that the *glmS* riboswitch is unique among riboswitch families, as it represents a metabolite-dependent ribozyme that undergoes self-cleavage upon recognition of glucosamine-6-phosphate (GlcN6P) (47, 48). In contrast to the findings for  $\Delta$ IP4 with induction by vancomycin, the  $\Delta$ IP5 and Mu50 VISA strains showed the upregulation of the *gntR*, *gntP*, *gntK*, and *ndk* genes instead of the *glmS* gene and the downregulation of the *cmk* and *pyr* genes (described above), which are associated with the thickness of the cell wall and the size of the UTP and UMP pool (49).

The gluconate (*gnt*) operon of *Bacillus subtilis* includes the *gntR*, *gntK*, *gntP*, and *gntZ* genes, encoding the transcriptional repressor of the operon, gluconate kinase, the gluconate permease, and an unidentified open reading frame, respectively (50).

GntR is classified in the GntR/DeoR family, which includes the Gnt-like protein LacR, and LacR is involved in the repression of the genes for lactose and fructose in *Lactococcus lactis* (51). Also, the GntR family repressor YtrA responds to the cell wall antibiotics ramoplanin and moenomycin, which are involved in binding to the substrate lipid II and the transglycosylase enzyme, respectively, in *Bacillus subtilis* (52). In the case of *S. aureus*, it has been reported that the GntR-like protein NorG, which positively affects the transcription of global regulators, has been shown to affect *S. aureus* genes involved in resistance to quinolones and  $\beta$ -lactams, such as genes encoding the NorB and AbcA transporters (53). It is possible that the Gnt operon might be related to cell wall metabolism in  $\Delta$ IP5 and Mu50; however, the role of the Gnt operon is unknown.

The *ndk* gene encodes nucleoside diphosphate kinase, catalyzes the synthesis of the nucleoside triphosphates UTP and CTP, and then maintains intracellular triphosphate pools in *E. coli* (54). The loss of function of Ndk in *E. coli* results in an increased rate of appearance of rifampin-resistant strains and an imbalance in deoxynucleoside triphosphate pool levels, and Ndk prevents the accumulation of dUTP in the cell (55). It seems that the size of the UTP pool increased.

In fact, we also reported that the *cmk* mutation leads to a thickening of cell wall peptidoglycan layers, increasing vancomycin resistance (17). When a metabolomics analysis between hVISA Mu3 and slow VISA Mu3-6R was performed, the amounts of UDP, UTP, and UDP-*N*-acetylglucosamine (UDP-GlcNAc) produced from GlcNAc-1P and UTP (56) were increased and the amount of GlcNAc-1P was decreased in Mu3-6R (Y. Katayama, unpublished data). Therefore, we suppose that the increase in the amount of UTP in the cell promotes cell wall synthesis.

In conclusion, this study provides new and important information on the functional significance of the mechanism responsible for increased resistance to vancomycin in strains of the Mu50 type. All six mutated genes required for acquisition of the VISA phenotype were directly or indirectly involved in the regulation of cell physiology. VISA seemed to be achieved through multiple genetic events accompanying drastic changes in cell physiology.

## ACKNOWLEDGMENTS

This work was supported by a Grant-in-Aid for Young Scientists B (24791029), a Grant-in-Aid for Scientific Research C (15K09581), and grant S1201013 from the Ministry of Education, Culture, Sports, Science and Technology Japan (MEXT) to the Foundation of Strategic Research Projects in Private Universities.

We thank Mitutaka Yoshida (Division of Ultrastructural Research, Juntendo University) for invaluable help with sample preparation and technical support with transmission electron microscopy.

## FUNDING INFORMATION

This work, including the efforts of Yuki Katayama, was funded by The Ministry of Education, Culture, Sports, Science and Technology Japan (Young Scientists B 24791029 and Research C 15K09581). This work, including the efforts of Keiichi Hiramatsu, was funded by The Ministry of Education, Culture, Sports, Science and Technology Japan (S1201013).

## REFERENCES

- Hanaki H, Kuwahara-Arai K, Boyle-Vavra S, Daum RS, Labischinski H, Hiramatsu K. 1998. Activated cell wall synthesis is associated with vancomycin resistance in methicillin-resistant *Staphylococcus aureus* clinical strains Mu3 and Mu50. *J Antimicrob Chemother* 42:199–209. <http://dx.doi.org/10.1093/jac/42.2.199>.
- Cui L, Murakami H, Kuwahara-Arai K, Hanaki H, Hiramatsu K. 2000. Contribution of a thickened cell wall and its glutamine nonamidated component to the vancomycin resistance expressed by *Staphylococcus aureus* Mu50. *Antimicrob Agents Chemother* 44:2276–2285. <http://dx.doi.org/10.1128/AAC.44.9.2276-2285.2000>.
- Cui L, Lian JQ, Neoh HM, Reyes E, Hiramatsu K. 2005. DNA microarray-based identification of genes associated with glycopeptide resistance in *Staphylococcus aureus*. *Antimicrob Agents Chemother* 49:3404–3413. <http://dx.doi.org/10.1128/AAC.49.8.3404-3413.2005>.
- Sieradzki K, Tomasz A. 2006. Inhibition of the autolytic system by vancomycin causes mimicry of vancomycin-intermediate *Staphylococcus aureus*-type resistance, cell concentration dependence of the MIC, and antibiotic tolerance in vancomycin-susceptible *S. aureus*. *Antimicrob Agents Chemother* 50:527–533. <http://dx.doi.org/10.1128/AAC.50.2.527-533.2006>.
- Smith TL, Pearson ML, Wilcox KR, Cruz C, Lancaster MV, Robinson-Dunn B, Tenover FC, Zervos MJ, Band JD, White E, Jarvis WR. 1999. Emergence of vancomycin resistance in *Staphylococcus aureus*. Glycopeptide-Intermediate *Staphylococcus aureus* Working Group. *N Engl J Med* 340:493–501.
- Matsuo M, Cui L, Kim J, Hiramatsu K. 2013. Comprehensive identification of mutations responsible for heterogeneous vancomycin-intermediate *Staphylococcus aureus* (hVISA)-to-VISA conversion in laboratory-generated VISA strains derived from hVISA clinical strain Mu3. *Antimicrob Agents Chemother* 57:5843–5853. <http://dx.doi.org/10.1128/AAC.00425-13>.
- McCallum N, Spehar G, Bischoff M, Berger-Bachi B. 2006. Strain dependence of the cell wall-damage induced stimulon in *Staphylococcus aureus*. *Biochim Biophys Acta* 1760:1475–1481. <http://dx.doi.org/10.1016/j.bbagen.2006.06.008>.
- Utaiida S, Dunman PM, Macapagal D, Murphy E, Projan SJ, Singh VK, Jayaswal RK, Wilkinson BJ. 2003. Genome-wide transcriptional profiling of the response of *Staphylococcus aureus* to cell wall-active antibiotics reveals a cell wall-stress stimulon. *Microbiology* 149:2719–2732. <http://dx.doi.org/10.1099/mic.0.26426-0>.
- Kuroda M, Kuroda H, Oshima T, Takeuchi F, Mori H, Hiramatsu K. 2003. Two-component system VraSR positively modulates the regulation of cell wall biosynthesis pathway in *Staphylococcus aureus*. *Mol Microbiol* 49:807–821.
- Katayama Y, Murakami-Kuroda H, Cui L, Hiramatsu K. 2009. Selection of heterogeneous vancomycin-intermediate *Staphylococcus aureus* by imipenem. *Antimicrob Agents Chemother* 53:3190–3196. <http://dx.doi.org/10.1128/AAC.00834-08>.
- Yamakawa J, Aminaka M, Okuzumi K, Kobayashi H, Katayama Y, Kondo S, Nakamura A, Oguri T, Hori S, Cui L, Ito T, Jin J, Kurosawa H, Kaneko K, Hiramatsu K. 2012. Heterogeneously vancomycin-intermediate *Staphylococcus aureus* (hVISA) emerged before the clinical introduction of vancomycin in Japan: a retrospective study. *J Infect Chemother* 18:406–409. <http://dx.doi.org/10.1007/s10156-011-0330-2>.
- Kato Y, Suzuki T, Ida T, Maebashi K. 2010. Genetic changes associated with glycopeptide resistance in *Staphylococcus aureus*: predominance of amino acid substitutions in YvqF/VraSR. *J Antimicrob Chemother* 65:37–45. <http://dx.doi.org/10.1093/jac/dkp394>.
- Hiramatsu K, Aritaka N, Hanaki H, Kawasaki S, Hosoda Y, Hori S, Fukuchi Y, Kobayashi I. 1997. Dissemination in Japanese hospitals of strains of *Staphylococcus aureus* heterogeneously resistant to vancomycin. *Lancet* 350:1670–1673. [http://dx.doi.org/10.1016/S0140-6736\(97\)07324-8](http://dx.doi.org/10.1016/S0140-6736(97)07324-8).
- Cui L, Neoh HM, Shoji M, Hiramatsu K. 2009. Contribution of vraSR and graSR point mutations to vancomycin resistance in vancomycin-intermediate *Staphylococcus aureus*. *Antimicrob Agents Chemother* 53:1231–1234. <http://dx.doi.org/10.1128/AAC.01173-08>.
- Ohta T, Hiramatsu K, Morikawa K, Maruyama A, Inose Y, Yamashita A, Oshima K, Kuroda M, Hattori M, Hiramatsu K, Kuhara S, Hayashi H. 2004. Nucleotide substitutions in *Staphylococcus aureus* strains, Mu50, Mu3, and N315. *DNA Res* 11:51–56. <http://dx.doi.org/10.1093/dnares/11.1.51>.
- Neoh HM, Cui L, Yuzawa H, Takeuchi F, Matsuo M, Hiramatsu K. 2008. Mutated response regulator graR is responsible for phenotypic conversion of *Staphylococcus aureus* from heterogeneous vancomycin-intermediate resistance to vancomycin-intermediate resistance. *Antimicrob Agents Chemother* 52:45–53. <http://dx.doi.org/10.1128/AAC.00534-07>.
- Cheung AL, Bayer AS, Yeaman MR, Xiong YQ, Waring AJ, Memmi G, Donegan N, Chaili S, Yang SJ. 2014. Site-specific mutation of the sensor kinase GraS in *Staphylococcus aureus* alters the adaptive response to distinct cationic antimicrobial peptides. *Infect Immun* 82:5336–5345. <http://dx.doi.org/10.1128/IAI.02480-14>.
- Matsuo M, Hishinuma T, Katayama Y, Cui L, Kapi M, Hiramatsu K. 2011. Mutation of RNA polymerase beta subunit (rpoB) promotes hVISA-to-VISA phenotypic conversion of strain Mu3. *Antimicrob Agents Chemother* 55:4188–4195. <http://dx.doi.org/10.1128/AAC.00398-11>.
- Saito M, Katayama Y, Hishinuma T, Iwamoto A, Aiba Y, Kuwahara-Arai K, Cui L, Matsuo M, Aritaka N, Hiramatsu K. 2014. “Slow VISA,” a novel phenotype of vancomycin resistance, found in vitro in heterogeneous vancomycin-intermediate *Staphylococcus aureus* strain Mu3. *Antimicrob Agents Chemother* 58:5024–5035. <http://dx.doi.org/10.1128/AAC.02470-13>.
- Hiramatsu K, Katayama Y, Matsuo M, Sasaki T, Morimoto Y, Sekiguchi A, Baba T. 2014. Multi-drug-resistant *Staphylococcus aureus* and future chemotherapy. *J Infect Chemother* 20:593–601. <http://dx.doi.org/10.1016/j.jiac.2014.08.001>.
- Cui L, Isii T, Fukuda M, Ochiai T, Neoh HM, Camargo IL, Watanabe Y, Shoji M, Hishinuma T, Hiramatsu K. 2010. An RpoB mutation confers dual heteroresistance to daptomycin and vancomycin in *Staphylococcus aureus*. *Antimicrob Agents Chemother* 54:5222–5233. <http://dx.doi.org/10.1128/AAC.00437-10>.
- Hiramatsu K, Katayama Y, Matsuo M, Aiba Y, Saito M, Hishinuma T, Iwamoto A. 2014. Vancomycin-intermediate resistance in *Staphylococcus aureus*. *J Global Antimicrob Resist* 2:213–224. <http://dx.doi.org/10.1016/j.jgar.2014.04.006>.
- Kuwahara-Arai K, Kondo N, Hori S, Tateda-Suzuki E, Hiramatsu K. 1996. Suppression of methicillin resistance in a *mecl*-containing pre-methicillin-resistant *Staphylococcus aureus* strain is caused by the *mecl*-mediated repression of PBP 2' production. *Antimicrob Agents Chemother* 40:2680–2685.
- Kawai Y, Marles-Wright J, Cleverley RM, Emmins R, Ishikawa S, Kuwano M, Heinz N, Bui NK, Hoyland CN, Ogasawara N, Lewis RJ, Vollmer W, Daniel RA, Errington J. 2011. A widespread family of bacterial cell wall assembly proteins. *EMBO J* 30:4931–4941. <http://dx.doi.org/10.1038/emboj.2011.358>.
- Chan YG, Frankel MB, Dengler V, Schneewind O, Missiakas D. 2013. *Staphylococcus aureus* mutants lacking the LytR-CpsA-Psr family of enzymes release cell wall teichoic acids into the extracellular medium. *J Bacteriol* 195:4650–4659. <http://dx.doi.org/10.1128/JB.00544-13>.
- Biswas R, Martinez RE, Gohring N, Schlag M, Josten M, Xia G, Hegler F, Gekeler C, Gleske AK, Gotz F, Sahl HG, Kappler A, Peschel A. 2012. Proton-binding capacity of *Staphylococcus aureus* wall teichoic acid and its role in controlling autolysin activity. *PLoS One* 7:e41415. <http://dx.doi.org/10.1371/journal.pone.0041415>.

27. Kajimura J, Fujiwara T, Yamada S, Suzawa Y, Nishida T, Oyamada Y, Hayashi I, Yamagishi J, Komatsuzawa H, Sugai M. 2005. Identification and molecular characterization of an *N*-acetylmuramyl-L-alanine amidase Sle1 involved in cell separation of *Staphylococcus aureus*. *Mol Microbiol* 58:1087–1101. <http://dx.doi.org/10.1111/j.1365-2958.2005.04881.x>.
28. Frankel MB, Schneewind O. 2012. Determinants of murein hydrolase targeting to cross-wall of *Staphylococcus aureus* peptidoglycan. *J Biol Chem* 287:10460–10471. <http://dx.doi.org/10.1074/jbc.M111.336404>.
29. Atilano ML, Pereira PM, Yates J, Reed P, Veiga H, Pinho MG, Filipe SR. 2010. Teichoic acids are temporal and spatial regulators of peptidoglycan cross-linking in *Staphylococcus aureus*. *Proc Natl Acad Sci U S A* 107:18991–18996. <http://dx.doi.org/10.1073/pnas.1004304107>.
30. Cui L, Iwamoto A, Lian JQ, Neoh HM, Maruyama T, Horikawa Y, Hiramatsu K. 2006. Novel mechanism of antibiotic resistance originating in vancomycin-intermediate *Staphylococcus aureus*. *Antimicrob Agents Chemother* 50:428–438. <http://dx.doi.org/10.1128/AAC.50.2.428-438.2006>.
31. Sieradzki K, Tomasz A. 2003. Alterations of cell wall structure and metabolism accompany reduced susceptibility to vancomycin in an isogenic series of clinical isolates of *Staphylococcus aureus*. *J Bacteriol* 185:7103–7110. <http://dx.doi.org/10.1128/JB.185.24.7103-7110.2003>.
32. Katayama Y, Zhang HZ, Hong D, Chambers HF. 2003. Jumping the barrier to beta-lactam resistance in *Staphylococcus aureus*. *J Bacteriol* 185:5465–5472. <http://dx.doi.org/10.1128/JB.185.18.5465-5472.2003>.
33. Katayama Y, Takeuchi F, Ito T, Ma XX, Ui-Mizutani Y, Kobayashi I, Hiramatsu K. 2003. Identification in methicillin-susceptible *Staphylococcus hominis* of an active primordial mobile genetic element for the staphylococcal cassette chromosome *mec* of methicillin-resistant *Staphylococcus aureus*. *J Bacteriol* 185:2711–2722. <http://dx.doi.org/10.1128/JB.185.9.2711-2722.2003>.
34. Bae T, Schneewind O. 2006. Allelic replacement in *Staphylococcus aureus* with inducible counter-selection. *Plasmid* 55:58–63. <http://dx.doi.org/10.1016/j.plasmid.2005.05.005>.
35. Gustafson JE, Berger-Bachi B, Strassle A, Wilkinson BJ. 1992. Autolysis of methicillin-resistant and -susceptible *Staphylococcus aureus*. *Antimicrob Agents Chemother* 36:566–572. <http://dx.doi.org/10.1128/AAC.36.3.566>.
36. Cui L, Ma X, Sato K, Okuma K, Tenover FC, Mamizuka EM, Gemmell CG, Kim MN, Ploy MC, El-Sohl N, Ferraz V, Hiramatsu K. 2003. Cell wall thickening is a common feature of vancomycin resistance in *Staphylococcus aureus*. *J Clin Microbiol* 41:5–14. <http://dx.doi.org/10.1128/JCM.41.1.5-14.2003>.
37. Rossi J, Bischoff M, Wada A, Berger-Bachi B. 2003. MsrR, a putative cell envelope-associated element involved in *Staphylococcus aureus* sarA attenuation. *Antimicrob Agents Chemother* 47:2558–2564. <http://dx.doi.org/10.1128/AAC.47.8.2558-2564.2003>.
38. Hubscher J, McCallum N, Sifri CD, Majcherczyk PA, Entenza JM, Heusser R, Berger-Bachi B, Stutzmann Meier P. 2009. MsrR contributes to cell surface characteristics and virulence in *Staphylococcus aureus*. *FEMS Microbiol Lett* 295:251–260. <http://dx.doi.org/10.1111/j.1574-6968.2009.01603.x>.
39. Over B, Heusser R, McCallum N, Schulthess B, Kupferschmid P, Gaiani JM, Sifri CD, Berger-Bachi B, Stutzmann Meier P. 2011. LytR-CpsA-Psr proteins in *Staphylococcus aureus* display partial functional redundancy and the deletion of all three severely impairs septum placement and cell separation. *FEMS Microbiol Lett* 320:142–151. <http://dx.doi.org/10.1111/j.1574-6968.2011.02303.x>.
40. Chan YG, Kim HK, Schneewind O, Missiakas D. 2014. The capsular polysaccharide of *Staphylococcus aureus* is attached to peptidoglycan by the LytR-CpsA-Psr (LCP) family of enzymes. *J Biol Chem* 289:15680–15690. <http://dx.doi.org/10.1074/jbc.M114.567669>.
41. Watanabe Y, Cui L, Katayama Y, Kozue K, Hiramatsu K. 2011. Impact of *rpoB* mutations on reduced vancomycin susceptibility in *Staphylococcus aureus*. *J Clin Microbiol* 49:2680–2684. <http://dx.doi.org/10.1128/JCM.02144-10>.
42. Matsuo M, Hishinuma T, Katayama Y, Hiramatsu K. 2015. A mutation of RNA polymerase  $\beta'$  subunit (RpoC) converts heterogeneously vancomycin-intermediate *Staphylococcus aureus* (hVISA) into “slow VISA.” *Antimicrob Agents Chemother* 59:4215–4225. <http://dx.doi.org/10.1128/AAC.00135-15>.
43. Aedo S, Tomasz A. 2016. The role of the stringent stress response in the antibiotic resistance phenotype of methicillin-resistant *Staphylococcus aureus*. *Antimicrob Agents Chemother* 60:2311–2317. <http://dx.doi.org/10.1128/AAC.02697-15>.
44. Nicoloff H, Elagoz A, Arsene-Ploetze F, Kammerer B, Martinussen J, Bringel F. 2005. Repression of the *pyr* operon in *Lactobacillus plantarum* prevents its ability to grow at low carbon dioxide levels. *J Bacteriol* 187:2093–2104. <http://dx.doi.org/10.1128/JB.187.6.2093-2104.2005>.
45. Lu Y, Switzer RL. 1996. Transcriptional attenuation of the *Bacillus subtilis* *pyr* operon by the *PyrR* regulatory protein and uridine nucleotides in vitro. *J Bacteriol* 178:7206–7211.
46. Lu Y, Turner RJ, Switzer RL. 1996. Function of RNA secondary structures in transcriptional attenuation of the *Bacillus subtilis* *pyr* operon. *Proc Natl Acad Sci U S A* 93:14462–14467. <http://dx.doi.org/10.1073/pnas.93.25.14462>.
47. Lunse CE, Schmidt MS, Wittmann V, Mayer G. 2011. Carba-sugars activate the *glmS*-riboswitch of *Staphylococcus aureus*. *ACS Chem Biol* 6:675–678. <http://dx.doi.org/10.1021/cb200016d>.
48. Watson PY, Fedor MJ. 2011. The *glmS* riboswitch integrates signals from activating and inhibitory metabolites in vivo. *Nat Struct Mol Biol* 18:359–363. <http://dx.doi.org/10.1038/nsmb.1989>.
49. Fricke J, Neuhaard J, Kelln RA, Pedersen S. 1995. The *cmk* gene encoding cytidine monophosphate kinase is located in the *rpsA* operon and is required for normal replication rate in *Escherichia coli*. *J Bacteriol* 177:517–523.
50. Fujita Y, Fujita T. 1987. The gluconate operon *gnt* of *Bacillus subtilis* encodes its own transcriptional negative regulator. *Proc Natl Acad Sci U S A* 84:4524–4528. <http://dx.doi.org/10.1073/pnas.84.13.4524>.
51. Barriere C, Veiga-da-Cunha M, Pons N, Guedon E, van Hijum SA, Kok J, Kuipers OP, Ehrlich DS, Renault P. 2005. Fructose utilization in *Lactococcus lactis* as a model for low-GC gram-positive bacteria: its regulator, signal, and DNA-binding site. *J Bacteriol* 187:3752–3761. <http://dx.doi.org/10.1128/JB.187.11.3752-3761.2005>.
52. Salzberg LI, Luo Y, Hachmann AB, Mascher T, Helmann JD. 2011. The *Bacillus subtilis* GntR family repressor YtrA responds to cell wall antibiotics. *J Bacteriol* 193:5793–5801. <http://dx.doi.org/10.1128/JB.05862-11>.
53. Truong-Bolduc QC, Dunman PM, Eidem T, Hooper DC. 2011. Transcriptional profiling analysis of the global regulator NorG, a GntR-like protein of *Staphylococcus aureus*. *J Bacteriol* 193:6207–6214. <http://dx.doi.org/10.1128/JB.05847-11>.
54. Goswami SC, Yoon JH, Abramczyk BM, Pfeifer GP, Postel EH. 2006. Molecular and functional interactions between *Escherichia coli* nucleoside-diphosphate kinase and the uracil-DNA glycosylase Ung. *J Biol Chem* 281:32131–32139. <http://dx.doi.org/10.1074/jbc.M604937200>.
55. Nordman J, Wright A. 2008. The relationship between dNTP pool levels and mutagenesis in an *Escherichia coli* NDP kinase mutant. *Proc Natl Acad Sci U S A* 105:10197–10202. <http://dx.doi.org/10.1073/pnas.0802816105>.
56. Mengin-Lecreux D, van Heijenoort J. 1994. Copurification of glucosamine-1-phosphate acetyltransferase and *N*-acetylglucosamine-1-phosphate uridyltransferase activities of *Escherichia coli*: characterization of the *glmU* gene product as a bifunctional enzyme catalyzing two subsequent steps in the pathway for UDP-*N*-acetylglucosamine synthesis. *J Bacteriol* 176:5788–5795.